3-14-2010

Investigation of the Thermal Degradation of Polyurea: The Effect of Ammonium Polyphosphate and Expandable Graphite

Walid Awad
Marquette University, walid.awad@marquette.edu

Charles A. Wilkie
Marquette University, charles.wilkie@marquette.edu

Accepted version. *Polymer*, Vol. 51, No. 11 (May 14, 2010): 2277-2285. DOI.

Investigation of the Thermal Degradation of Polyurea: The Effect of Ammonium Polyphosphate and Expandable Graphite

Walid H. Awad
Department of Chemistry and Fire Retardant Research Facility, Marquette University
Milwaukee, WI

Charles A. Wilkie
Department of Chemistry and Fire Retardant Research Facility, Marquette University
Milwaukee, WI

Abstract:

Polyurea was compounded with ammonium polyphosphate and expandable graphite and the morphology was studied by atomic force microscopy. The thermal degradation of polyurea and polyurea compounded with the additives has been investigated using thermogravimetry coupled with Fourier Transform infrared spectroscopy and mass spectrometry. The study of the thermal degradation and the parameters affecting the thermal stability of PU is essential in order to effectively design flame retarded polyurea. In general, thermal decomposition of polyurea occurs in two steps assigned to the degradation of the hard segment and soft segment, respectively. Adding these additives accelerates the decomposition reaction of polyurea. However,

Polymer, Vol. 51, No. 11 (May 2010): pg. 2277-2285. DOI.

it is clear that more char is formed. This char is thermally more stable than the carbonaceous structure obtained from neat PU. The intumescent shield traps the polymer fragments and limits the evolution of small flammable molecules that are able to feed the flame.

Keywords: Polyurea, TGA/FTIR, Thermal analysis**.**

1. Introduction

Interest in the development of polyureas (PUs) has increased significantly due to their use as an impact-resistant coating system [1], [2], [3], [4], [5], [6], [7] and [8]. The properties of PU make it an attractive candidate for this type of application: the reaction of isocyanate with polyetheramine to form the material is very rapid, so that the coating properties are largely independent of ambient temperature and humidity. Polyureas have a microphase-separated segmented block copolymer morphology that consists of hard segment (HS) domains dispersed in a soft segment (SS) matrix. The hard domains are extensively hydrogen-bonded and function as both reversible physical cross-links and reinforcing filler, thus providing good mechanical properties, especially toughness [9].

One of the greatest impediments to the development and application of polyureas in the design and construction of military facilities is their relatively high flammability and their susceptibility to degradation due to exposure to elevated temperatures caused by fire [10], [11], [12] and [13]. One effective way to flame retard polyurea is to use an intumescent system. Intumescence can be described as fire retardant technology which causes an otherwise flammable material to foam, forming an insulating barrier when exposed to heat.

Common intumescent materials, which are effective with polyurea, are ammonium polyphosphate (APP) and expandable graphite (EG), as indicated in our previous papers [12] and [13]. APP is an effective intumescent fire retardant for several kinds of polymer-based materials and, in particular, for polyurethanes [14], [15], [16] and [17]. It is a high molecular weight chain phosphate, whose efficiency is generally attributed to an increase of char formation through a condensed phase reaction. On the other hand, expandable

graphite is a graphite intercalation compound. The special layer lattice structure of flake graphite makes it possible to be intercalated by other chemicals. When exposed to heat, EG expands and generates a voluminous insulating layer thus providing fire performance to the polymeric matrix [18], [19], [20], [21] and [22].

The study of the thermal decomposition of polyurea is essential to address the flammability issue. This study is important from both a fundamental and a technological perspective; the investigation of degradation processes allows for the determination of the optimum conditions for designing and processing PU as well as obtaining high-performance polymer with improved thermal stability. Therefore, it is essential to analyze the decomposition process in such a way that the different aspects involved are considered in a systematic manner.

It is worth noting that the thermal decomposition of polyurethane has received considerable attention in the literature [23], [24], [25], [26] and [27], but very little attention has been given to the thermal decomposition of polyurea. It is generally believed that the thermal degradation and stability of polyurethane is related to the hard segment and soft segment structures. The variation in the type and amount of these building blocks affects the thermal stability of the resultant product.

The aim of this study is to investigate the thermal decomposition of polyurea and its composite with ammonium polyphosphate and expandable graphite using TG-FTIR-MS. This system is a very powerful technique combining the direct measurement of mass loss as a function of temperature with the use of sensitive spectroscopic detectors FTIR and MS.

2. Experimental

2.1. Materials

The materials used throughout this work are: Isocyanate (Isonate 143L from Dow Chemical Company), Diamine (Versalink p-1000 from Air Products), Ammonium Polyphosphate APP, Phos-Chek P/30 (ICL Performance Products Inc) and Grafguard Expandable Graphite 160-80N (Graftech).

2.2. Sample preparation

The polyurea samples were prepared in a beaker by reacting four parts (by weight) of poly(tetramethylene oxide-di-*p*-aminobenzoate) (Versalink P-1000; Air Products) with 1 part of a polycarbodiimide-modified diphenylmethane diisocyanate (Isonate 143L; Dow Chemical). The diamine and diisocyanate undergo rapid linear polycondensation to yield a microphase-separated block copolymer having ca. 20% hard segments by mass (Fig. 1). For polyurea with APP and EG, the additive (5 wt% of the final polyurea) is mixed first in the diamine for several minutes. The dispersion of the additives was achieved using mechanical mixing followed by ultrasonication. Then, the isocyanate was added to the mixture with continuous stirring for 1 min, and the contents of the beaker were poured into a mold. The samples were cured at room temperature for 12 h, and then were placed in a vacuum oven at 70 °C for additional 24 h.

2.3. Instrumentation

2.3.1. TG-FTIR-MS

The samples were investigated using simultaneous thermogravimetry (Netzsch TG 209 F1 Iris) coupled with mass spectrometry (QMS Aeolos) and FTIR (Bruker Tensor 27). The analyses were performed under flowing nitrogen at 20 mL/min. The TG resolution is 0.1 µg. The sample size was 20 mg and the heating rate was 10 °C/min from room temperature to 600 °C. The mass spectra was measured in the range from 1 to 300 amu using quadrupole mass filter electron impact ionization. The coupling system between TG, FTIR and MS was heated at 200 °C to prevent condensation of evolved gases.

2.3.2. Atomic force microscopy (AFM)

Tapping mode AFM was performed with an Innova Scanning Probe system from Veeco. Topographic (height) and phase images were recorded simultaneously under ambient conditions. Silicon nitride, Si_3N_4, cantilever probes with a nominal tip radius of 5–10 nm and spring constant in the range of 20–100 N/m were oscillated at their fundamental resonance frequencies, which ranged between 250

and 300 kHz. All data were collected with 256 × 256 pixels per image. Typical scan rate and set-point amplitude ratio during recording were 1.0 Hz and 3.0–4.0 V, respectively.

2.3.3. Differential scanning calorimeter

The thermal phase behavior of polyurea was investigated using Netzsch instrument 200 F3 Maia differential scanning calorimeter, operating at a heating and cooling rate of 10 °C/min under a nitrogen atmosphere. Polyurea samples were subjected to two heating and cooling cycles between −70 and 250 °C. Transitions were investigated during the second heating and cooling cycles.

3. Results and discussion

3.1. Morphology of polyurea

Polyurea have been used in a wide range of protective coating applications. Although polymer composition varies with different products, a urea linkage covalently bonds 'hard' and 'soft' segments into a multi-block copolymer. The thermodynamic incompatibility of the HS and SS drives the polymer system into a two-phase morphology in which hydrogen-bonded, crystalline hard microdomains form amid the rubbery soft domains. The two-phase morphology provides the key to controlling performance and versatility in tuning properties by varying the composition or content of one or the other phase.

The properties of polyureas are well known to be largely dependent on their microphase-separated morphology to the extent that alterations in that phase separation can have dramatic effects. Therefore, in the interest of obtaining visual evidence of the microphase structure of polyurea, tapping mode AFM was employed. In this mode, the cantilever oscillates vertically near its resonance frequency so that the tip makes brief contact with the sample during each oscillation cycle. The level of tapping force used during imaging is related to the ratio of the set-point amplitude to the free-oscillation amplitude, hereafter called the set-point ratio. As the tip is brought into contact with the sample surface, changes occur in the probe oscillation including phase angle, amplitude, and frequency as a result of tip–sample interactions. A phase image is recorded based on the changes in phase angle as a constant amplitude is maintained. Phase

images for heterogeneous materials often reflect differences in the adhesive and/or mechanical properties of different phases or components.

Topographic and phase contrast images of virgin polyurea are shown in Fig. 2. The images provide direct visual evidence of two distinct phases: a well-dispersed, interconnected, hard phase embedded in a soft segment matrix. In typical phase images from tapping mode AFM, higher offsets are usually generated by interactions of the tip with materials of higher dynamic modulus; therefore, in Fig. 2 the darker areas correspond to the soft segment domain and the lighter areas correspond to the hard segment domain. For the topographic image, the overall height changes over the 50 × 50 μm area are small, with a peak-to-valley roughness of less than 0.8 μm.

3.2. Thermal characterization

The soft and hard domain thermal transitions of segmented polyurea samples were investigated using DSC. Second heating and cooling scan data were employed to detect these transitions (DSC curves not shown). The soft domains possess a low-temperature glass transition at −46 °C. The material showed an order–disorder transition centered at 143 °C (T_{ODT}), and the hard segment melting temperature at 161 °C.

3.3. Thermal degradation of polyurea

Coupling a TG instrument with evolved gas analyzers, such as FTIR and a mass spectrometer, produces a very powerful analytical technique that gives information from the thermal balance as well as compositional information from the spectrometers simultaneously. Determination of volatile products evolved during thermal degradation using TG-FTIR-MS analysis gives important information regarding the nature and mechanism of thermal decomposition. The TG-FTIR-MS apparatus consists of a sample suspended from a balance in a gas stream within a furnace and, once the sample is heated, volatile decomposition products are formed. The TG-FTIR-MS system has suitable interfaces to carry the gaseous decomposition products from the TG furnace to the detection system of FTIR and MS spectrometers, *i.e.* the method consists of carrying the evolving volatile products out

of the furnace directly into the FTIR gas cell and MS where the gases are analyzed.

3.3.1. TG measurement

Fig. 3, Fig. 4, Fig. 5, Fig. 6, Fig. 7 and Fig. 8 show the TG-FTIR-MS data of virgin polyurea under nitrogen atmosphere. The TG curve and its corresponding derivative mass loss curves (DTG) are shown in Fig. 3. As can be seen, the sample exhibited two degradation stages located ca. 322 and 408 °C. The mass losses for the first and second stages were 21 and 73% w/w, respectively. The first mass loss can be attributed to the degradation of hard segment because of the relatively low thermal stability of the urea group. The second mass loss is due to soft segment decomposition. The agreement between stoichiometry (20 wt% hard segment) and TGA measurement gives additional credence to the assertion that the first step is HS degradation while the second is degradation of the soft segment. The hard segments are less thermally stable, and their degradation will depend on the isocyanate nature. The decomposition process of polyurea ends with the formation of char residue (6 wt.%) and the evolution of all volatile species.

3.3.2. FTIR measurement

During TGA/FTIR experiments, spectral data are repeatedly collected in the form of interferograms and then processed to build up a Gram–Schmidt reconstruction, each point of which corresponds to the total IR absorbance of the evolved components in the range of 4000–650 cm^{-1}, *i.e.* the Gram–Schmidt plot is the result of averaging all FTIR peak intensities over the entire spectral range [28]. Thus, the total absorbance intensity of each mass loss is a function of the concentration of evolved gases and their corresponding infrared extinction coefficients. Fig. 4 shows the Gram–Schmidt plot for virgin polyurea.

Two evolved gas regions can be identified and they are related to the mass losses recorded in the DTG curve. It should be noted that the peaks in the Gram–Schmidt plot are shifted to higher temperatures than the corresponding DTG curve. This is due to the delay time between the gas generation and its detection in the FTIR equipment. The first peak observed in the Gram–Schmidt is small, suggesting that the amount of the evolved gases in this stage is low and with low

infrared extinction coefficients. In contrast, the second degradation stage seems to be composed of a considerable amount of evolved gases with high infrared extinction coefficients.

Fig. 5 shows 3D FTIR spectra for the gases produced from thermal degradation of virgin polyurea. The main evolved product of the first degradation step is carbon dioxide (with absorptions at 2359 and 669 cm^{-1}). The spectra also show a small peak at 2981 cm^{-1} that can be attributed to C–H stretching vibration. In contrast, the spectrum obtained during the second stage showed a strong absorption band at 2955 cm^{-1} which is the C–H stretching vibrations for methylene and methyl groups. Carbon dioxide with its characteristics absorption bands can be identified. A characteristic carbonyl absorption band at 1749 cm^{-1} and a band at 1105 cm^{-1} related to C=O vibration can also be observed.

3.3.3. MS measurement

The exact composition of the polyurea degradation products was determined by Thermogravimetry coupled to a Mass Spectrometer. Volatile degradation products in a controlled temperature treatment are directly transferred into the electron impact ion source of the MS via a fused silica capillary which is heated at 200 °C. The input gas is ionized by electron impact and then the ions are sent through a quadrupole mass filter and finally impacted onto a secondary electron multiplier producing an output current proportional to the ion current. All analyses were made from 50 to 600 °C at a rate of 10 °C/min under nitrogen atmosphere using samples of ca. 20 mg.

The volatilization profiles, represented as Single Ion Current, of the fragments originating in the thermal degradation of polyurea are shown in Fig. 6, Fig. 7 and Fig. 8. The mass spectrum range recorded was from 41 to 72 *m*/*z*; no peaks were observed at higher *m*/*z* values. The release of carbon dioxide during the first degradation stage was confirmed by a fragment at *m*/*z* 44; this signal was also observed in the second degradation stage. This supports the FTIR data where carbon dioxide has been observed in both stages, but it is much more pronounced in the first step of the degradation. The peaks at *m*/*z* 43 and 57, which appear with strong intensity in the second degradation step, can be assigned to groups with isocyanate end group (*i.e.* HNCO and CH_3NCO, respectively). The peaks at *m*/*z* 41, 42, 54 and 55, which

Polymer, Vol. 51, No. 11 (May 2010): pg. 2277-2285. DOI.

can be assigned to hydrocarbon fragments C_xH_y, start to appear in the first degradation step with low intensity, and continue to appear with high intensity in the second degradation step. All these data support the TG-FTIR findings.

3.4. Polyurea–ammonium polyphosphate composites

3.4.1. Morphology of polyurea/APP

Tapping mode AFM images were taken for the polyurea/ammonium polyphosphate sample. Topographic and phase contrast images are shown in Fig. 9. The overall height changes over the 5 × 5 μm area are small, with a peak-to-valley roughness of less than 0.2 μm. Because height changes are not related to the presence of APP particles, the APP particles are easier to discern in the phase contrast image compared to the topographic image. In the phase image, a large number of what appears to be APP particles can be observed. This morphology hints at good dispersion of APP particles in the polyurea matrix. The phase contrast in the image is likely caused by the repulsive tip–sample interactions with APP, resulting in darker areas or features, and an attractive tip–sample interaction with the polyurea, resulting in brighter areas.

3.4.2. Thermal degradation of polyurea/APP

3.4.2.1. TG measurement

Two degradation steps can be recognized in the thermal degradation of ammonium polyphosphate (data are not shown). The first step, which begins around 300 °C, consists essentially of elimination of NH_3 and H_2O, leading to the formation of a highly crosslinked polyphosphoric acid, whereas the second step, at a temperature higher than 550 °C, corresponds to polyphosphoric acid evaporation and/or dehydration to P_4O_{10} which sublimes [29].

Fig. 10 shows the TG and DTG curves of polyurea compounded with 5% ammonium polyphosphate. These data indicate that, similar to the virgin polyurea, the thermal degradation of PU in the presence of APP proceeds in two steps. However, the two degradation steps have been shifted to lower temperatures (ca. 298 and 357 °C). This clearly gives an indication of the destabilizing effect of APP on polyurea, which can be attributed to the acidic effect of APP. The

fraction of mass loss that corresponds to the first and second step is 25% and 65% respectively.

The char residue formed after complete evaporation of the evolved species is 10 wt%. These data indicate that APP slightly enhances the char formation. It is generally accepted that char yields as determined from TG experiments are an indirect way of measuring the fire retardant properties of polymers [30] and [31]. Char formation in a fire limits the amount of volatile fuel that can be produced by the burning polymer. Of course, the structure of the char is at least as important as its quantity. In general, char provides a thermally insulating layer or barrier at the surface of the burning polymer, reduces heat and mass transmission into the material and provides good insulation to the underlying combustible polymer from the heat and fire.

3.4.2.2. FTIR measurement

Gram–Schmidt thermograms provide information related to the overall quantitative distribution of the evolved gases during the thermal degradation. Two well defined degradation steps can be identified in the Gram–Schmidt plot of polyurea–APP (curves not shown).

3D FTIR spectra obtained during the degradation process of polyurea with ammonium polyphosphate are shown in Fig. 11. The two degradation steps of polyurea can be identified. Analysis of the data clearly shows that there are significant changes in the spectra as suggested by TG analysis. Two absorption peaks, at 918 and 1082 cm^{-1}, can be seen in the first degradation step and continue to appear with higher intensity in the second step. These peaks can be attributed to the absorption of phosphate species P–O–C, which would evolve if a phospho-carbonaceous structure is formed in the solid and then degrades. Also, the major peaks (absorption range 2870–2981 cm^{-1}) in the second degradation step can be ascribed to the volatilization of aliphatic carbon. The evolution of carbon dioxide in the first and second degradation steps is confirmed with absorptions at 2359 and 669 cm^{-1}.

These data demonstrate the formation of phospho-carbonaceous structure. With the addition of ammonium polyphosphate, the degradation of PU was accelerated, due to the formation of phosphoric

acid. In addition, the phosphoric acid could also crosslink and forms a stable solid on the surface. Therefore, the char yield increased and the remaining PU did not undergo further degradation.

3.4.2.3. MS measurement

The single ion current for the volatile species detected during the thermal degradation of polyurea compounded with ammonium polyphosphate are shown in Fig. 12, Fig. 13 and Fig. 14. The mass spectra profiles support the TG-FTIR data that the thermal degradation of polyurea with ammonium polyphosphate occurs in two degradation steps, with the main degradation products evolved in the second stage. Carbon dioxide can be identified (*m*/*z* 44) in both degradation steps. The peaks at *m*/*z* 43 and 57, corresponding to the isocyanate moieties HNCO and CH_3NCO, can be identified albeit with small intensity relative to that observed with virgin polyurea. The evolved hydrocarbon fragment can be observed at peaks *m*/*z* 41, 42, 53, 54, 71 and 72; these were all seen in the degradation of PU alone.

3.5. Polyurea–expandable graphite composites

3.5.1. Morphology of polyurea/expandable graphite

The surface morphology of polyurea compounded with 5% expandable graphite was probed using tapping mode AFM. Fig. 15 shows the phase contrast and the topographic images. The phase image reveals that good dispersion of expandable graphite in polyurea has occurred; the domains that appear as small islands are bright compared to the polyurea matrix. The size, dispersity, shape, and spacing of the domains vary over the sample surface. In the topographic image, these smaller features are not evident, possibly because any associated topographic changes are small relative to those of the large structures. The overall height changes over the 5 × 5 μm area, with a peak-to-valley roughness of less than 0.2 μm.

3.5.2. Thermal degradation of polyurea/EG

3.5.2.1. TG measurement

Expandable graphite is an intumescent flame retardant that can effectively improve the flame retardancy of polyurea. The essential property of expandable graphite is the onset of expansion temperature and the expansion volume. The decomposition of intercalated

compounds (e.g., H_2SO_4 decomposes to H_2O and SO_3 gas) as well as oxidation of EG by acid (H_2SO_4 oxidizes carbon and produces CO_2 and SO_2 around 220 °C) in the presence of heat produces pressure that ultimately increases the distance between the graphitic basal planes. Therefore, once exposed to heat, EG forms a low density worm-like thermal insulating layer structure on the surface of the PU that prevents heat and oxygen transfer and provides good fire retardant performance [20]. The blowing reaction is shown below:

$$C_{(s)} + 2H_2SO_{4(l)} \rightarrow CO_{2(g)} + 2H_2O_{(g)} + 2SO_{2(g)} \qquad (1)$$

Fig. 16 shows the TG curve and its corresponding derivative mass loss (DTG) of polyurea with 5% expandable graphite in nitrogen. Two degradation steps, similar to neat polyurea, can be recognized. The maximum rate of mass loss for the first degradation step occurs at 314 °C. This degradation step, which has been shifted to lower temperature compared to virgin polyurea, is due to the degradation of the hard segment and results in the formation of isocyanate and diamine. The second degradation step, which takes place in the temperature range 360–450 °C and has a maximal rate of mass loss at 407 °C, may be attributed to the degradation of the soft segment. It is clear that adding expandable graphite has a destabilizing effect on the thermal stability of polyurea, especially its first degradation step. This can be explained by the oxidizing effect of H_2SO_4 released from EG. The fraction of mass loss that corresponds to the first and second step is 25% and 64% respectively. The char residue at 600 °C is 10%.

3.5.2.2. FTIR measurement

Fig. 17 shows the FTIR spectra of the species evolved in the two degradation steps of polyurea compounded with expandable graphite. Analysis of the data suggests that there are changes to the spectra of polyurea after compounding with EG. The absorption peaks in the range 2860–2980 cm^{-1} observed in the first degradation step can be attributed to the volatilization of aliphatic carbon. This volatilization process continues in the second step with great intensity as shown in Fig. 17. The absorption peaks at 2359 and 669 cm^{-1}, which correspond to the evolution of carbon dioxide, appear in both the first and the second degradation steps. It should be noted that carbon dioxide is evolved in large quantities during the degradation of PU/EG. This may be explained by the reaction for the degradation of EG shown in

equation (1). The onset of degradation of sulfuric acid intercalated between the layers of expandable graphite and the evolution of sulfur dioxide appears in the first step in low quantities. This explains the decrease in the thermal stability of the first step. In the second step, large quantities of sulfur dioxide are produced. SO_2 shows a strong peak at 1100 cm^{-1} and a relatively broad but weak FTIR spectrum in the 1300–1400 cm^{-1} region; it suffers interferences from water absorption.

3.5.2.3. MS measurement

The total ion current (TIC) for the species evolved during the thermal degradation of PU/EG are shown in Fig. 18 and Fig. 19. The total ion current profiles for the two degradation steps have been shifted to higher temperatures, due to the delay time between the evolution of the fragment species and their detection by the mass spectrometer. A strong TIC is shown in Fig. 18 that corresponds to the moieties produced in the first step. On the other hand, many TIC peaks that span the temperature range 400–600 °C can be observed in the second step. Carbon dioxide at *m*/*z* 44 has been detected in both the first and second degradation steps. The *m*/*z* 64 fragment (SO_2) is produced from degradation of expandable graphite and starts to evolve in the first step and continues with significant intensity in the second step. This data supports the observation made by FTIR. Fragments at *m*/*z* 40, 41, 42, 45, 46 and 70 that can be assigned to hydrocarbon species have been detected mainly in the second degradation step. The isocyanate species have also been detected at *m*/*z* 43 and 56.

3.6. Comparison of polyurea and its composites

The AFM results show that both APP and EG are well-dispersed in the PU. Both additives destabilize the PU in that the onset of the degradation is earlier in the presence of the additive compared to the virgin PU; APP is somewhat more destabilizing than is EG, perhaps due to the acidity of the APP. At the same time, there is a small increase in the amount of char that is produced; the products of the degradation are the same in the virgin polymer as in that with additives. This suggests that the additives offer some physical mechanism of stabilization rather than a chemical process in which the degradation pathway is changed.

4. Conclusions

AFM images indicated the microphase-separated morphology of polyurea and provided visual evidence for the good dispersion of APP and EG in polyurea. The thermal decomposition of PU is a complex heterogeneous process. The hard and soft segment content and the degree to which they are separated play a vital role in the thermal stability of polyurea. In general, the thermal degradation of polyurea involves two steps. The first, and least stable, step, which corresponds to the degradation of the hard segment, leads to the release of the trapped volatile materials. The second, and most stable, step corresponds to the soft segment degradation and results in mass loss and degradation of mechanical properties. Finally a complete thermal breakdown of the chains yields a mixture of CO, CO_2, HNCO, CH_3NCO, simple hydrocarbons and a complex char.

Adding APP and EG has a destabilizing effect on the degradation process of polyurea, but the char yield was increased. This char is composed of a carbonaceous structure which is thermally more stable than the carbonaceous structure obtained for virgin PU. At high temperature, the char layer formed on the surface provides resistance to heat and mass transfer, giving good heat insulation to the underlying polyurea. Therefore, an intumescent system shields the underlying PU from heat and fire. This lowers the temperature of the PU surface beneath the char and causes a lag in the surface temperature rise. Additionally, the char layer hinders the diffusion of oxygen to the PU surface.

Acknowledgment

The work was financially supported by the US Air Force under grant number FA8650-07-1-5901.

References

1. Yi J, Boyce MC, Lee GF, Balizer E. Polymer 2006;47:319.

2. Chakkarapani V, Ravi-Chandar K, Liechti KM. J Eng Mater Technol 2006;128:489.

3. Roland CM, Twigg JN, Vu Y, Mott PH. Polymer 2007;48:574.

4. Roland CM, Casalini R. Polymer 2007;48:5747.

5. Sarva SS, Deschanel S, Boyce M, Chen W. Polymer 2007;48:2208.

6. Xue Z, Hutchinson JW. Mech Mater 2007;39:473.

7. Tekalur SA, Shukla A, Shivakumar K. Comput Struct 2008;84:271.

8. http://www.pda-online.org.

9. Das S, Yilgor I, Yilgor E, Wilkes GL. Polymer 2008;49:174.

10. Koo JH, Muskopf B, Venumbaka S, Van Dine R, Spencer B, Sorathia U. In: Proceedings of the 32nd International SAMPE Technical Conference. Paper No. 136; 2000.

11. Sorathia U, Gracik T, Ness J, Durkin A, Williams F, Hunstad M, et al. J Fire Sci 2003;24:433.

12. Costache MC, Kanugh EM, Sorathia U, Wilkie CA. J Fire Sci 2006;24:433.

13. Awad HW, Nyambo C, Kim S, Dinan RJ, Fisher JW, Wilkie CA. In: Wilkie CA, Morgan AB, Nelson GL, editors. Fire and polymers V, materials and concepts for fire retardancy. ACS Symposium Series 1013; 2009. p. 102-17.

14. Papa AJ. In: Kuryla WC, Papa AJ, editors. Flame retardancy of polymeric materials, vol. 3. New York: Marcel Dekker; 1975. p. 1.

15. Siat C, Bourbigot S, Le Bras M. In: Lewin M, editor. Recent advances in flame retardancy of polymeric materials, vol. 7. Norwalk, CT: BCC; 1997. p. 318.

16. Mount RA, Pysz JF. Proc Int Conf Fire Saf 1991;16:203.

17. Duquesne S, Le Bras M, Bourbigot S, Delobel R, Camino G, Eling B, et al. J Appl Polym Sci 2001;82:3262.

18. Uhl FM, Yao Q, Wilkie CA. Polym Adv Technol 2005;16:533.

19. Uhl FM, Yao Q, Nakajima H, Manias E, Wilkie CA. Polym Degrad Stab 2002;76:111.

20. Duquesne1 S, Le Bras M, Bourbigot S, Delobel R, Vezin H, Camino G, et al. Fire Mater 2003;27:103-17.

21. Penszek P, Ostrysz R, Krassowski D. Flame Retardants 2000. London, UK; 8e9 February, 1999. p. 105-11.

22. Krassowski DW, Hutchings DA, Quershi SP. Fire retardant chemicals association. Fall Meeting, Naples, FL; 1996. p. 137-46.

23. Petrovic ZS, Zavargo Z, Flynn JH, Macknight WJ. J Appl Polym Sci 1994;51:1087-95.

24. Lee HK, Ko SW. J Appl Polym Sci 1993;50:1269-80.

25. Lage LG, Kawano Y. J Appl Polym Sci 2001;79:910-9.

26. Liu J, Ma D. J Appl Polym Sci 2002;84:2206-15.

27. Pielichowski K, S1otwinska D, Dziwinski E. J Appl Polym Sci 2004;91:3214-24.

28. Marini A, Berbenni V, Capsoni D, Riccardi R, Zerlia T. Appl Spectrosc 1994;48:1468-71.

29. Camino G, Costa L, Trossarelli L. Polym Degrad Stab 1984;6:243-52.

30. Van Krevelen DW. Properties of polymers, vol. 28. NY: Elsevier Scientific; 1976 [Chapter 26B].

31. Lyon RE. Polym Degrad Stab 1998;61:201.

About the Authors

Charles A. Wilkie : Department of Chemistry and Fire Retardant Research Facility, Marquette University, P.O. Box 1881, Milwaukee, WI 53201, United States

Email: charles.wilkie@marquette.edu

Appendix

Fig. 1: Structure of Segmented Polyurea

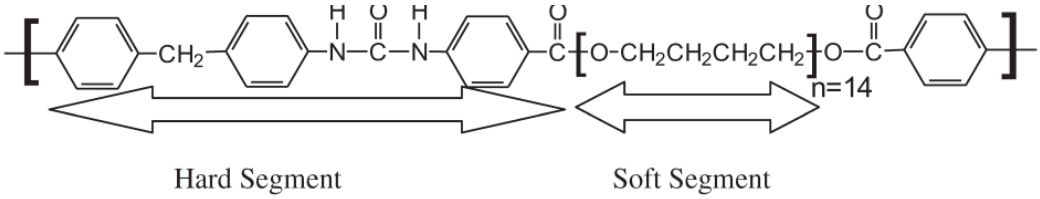

Fig. 2: Tapping Mode AFM Images of Neat Polyurea Sample

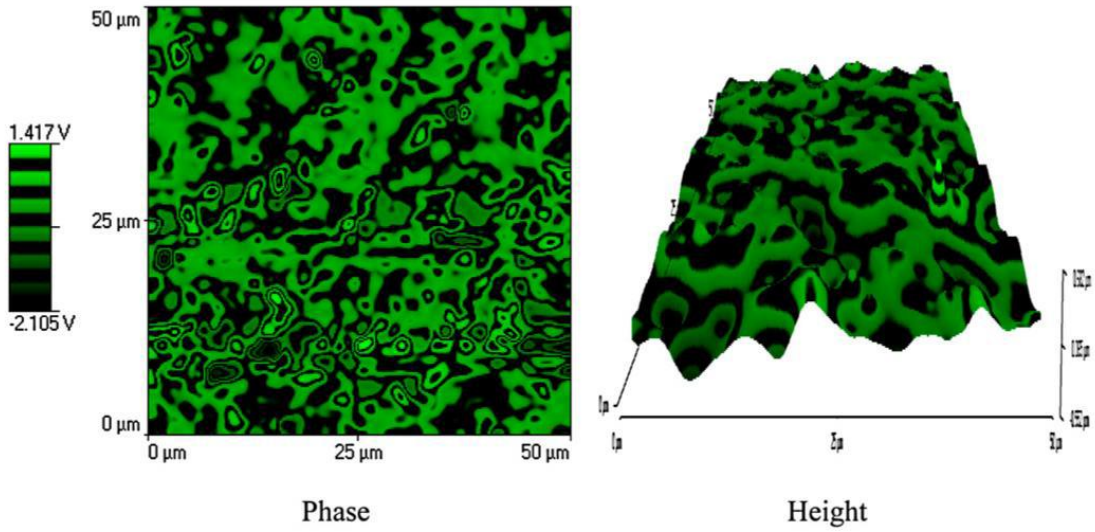

The left image is the phase contrast image while the right image is the height or topgraphic image.

Polymer, Vol. 51, No. 11 (May 2010): pg. 2277-2285. DOI.

Fig. 3: TG and DTG of Virgin Polyurea under Nitrogen Atmosphere

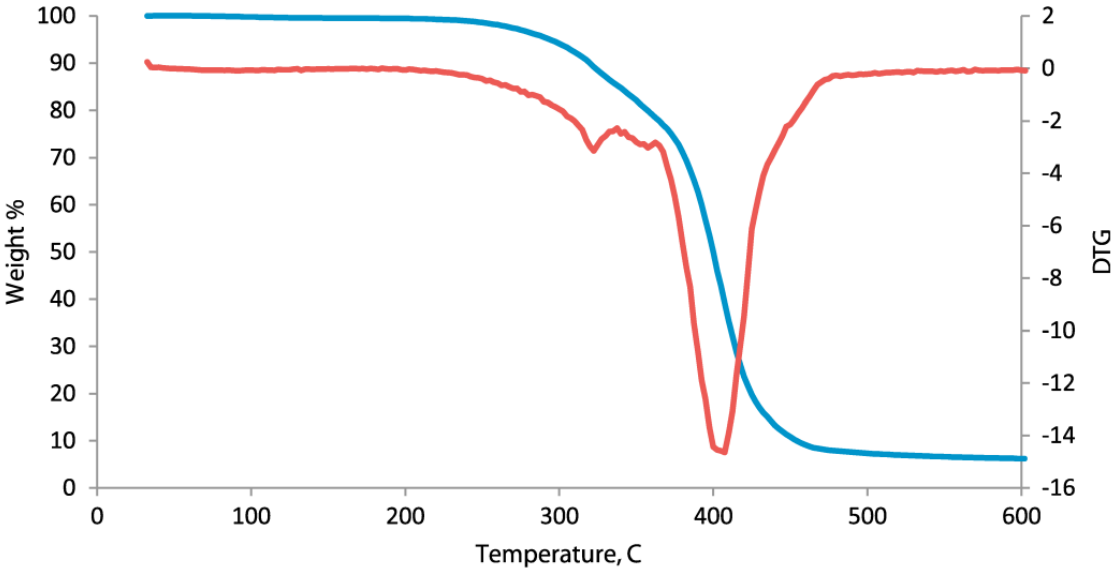

Fig. 4: Gram–Schmidt Plot of Virgin Polyurea

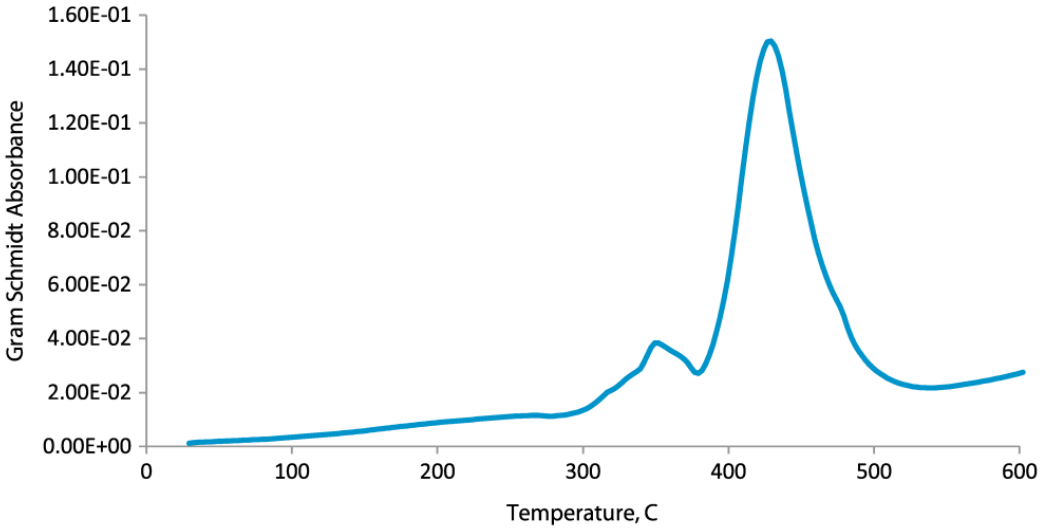

Fig. 5: 3D Diagram Corresponding to Gases Evolved from Degradation of Virgin Polyurea in the Temperature Range 30–600 °C

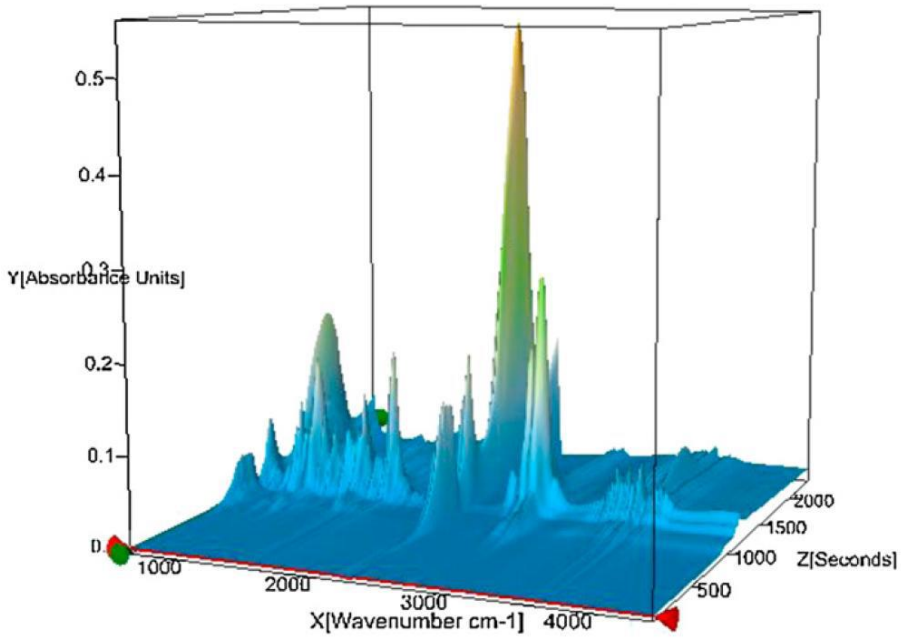

Fig. 6: Single Ion Current Curves for Species Produced from Degradation of Polyurea

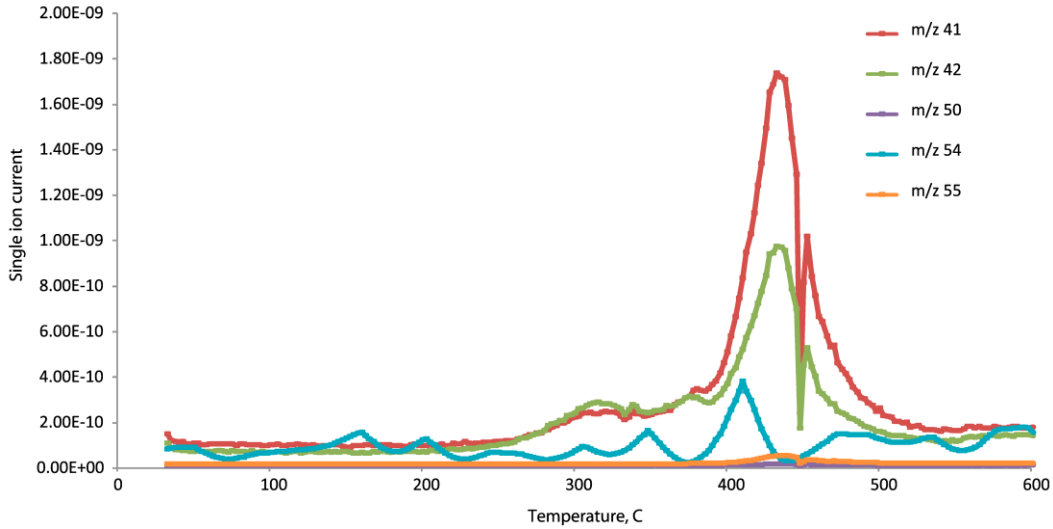

Fig. 7: Single Ion Current Curves for Species Produced from Degradation of Polyurea

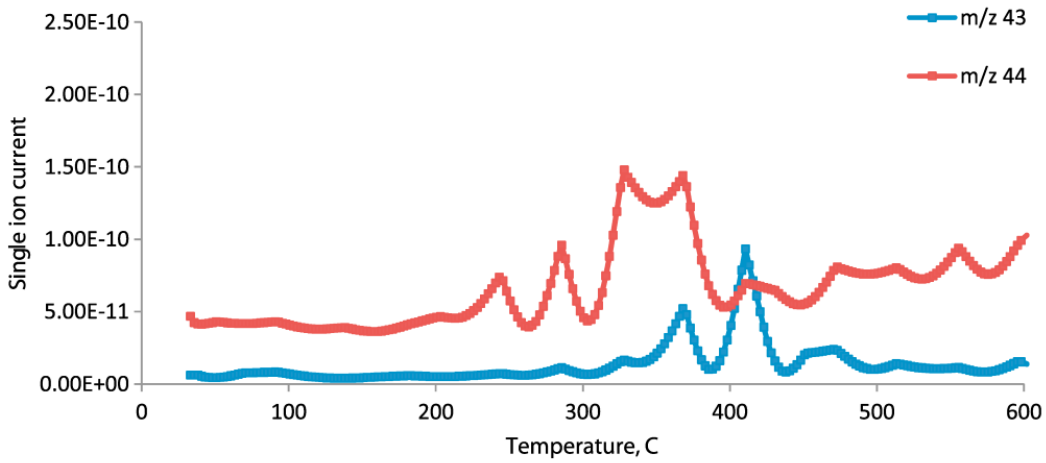

Fig. 8: Single Ion Current Curves for Species Produced from Degradation of Polyurea

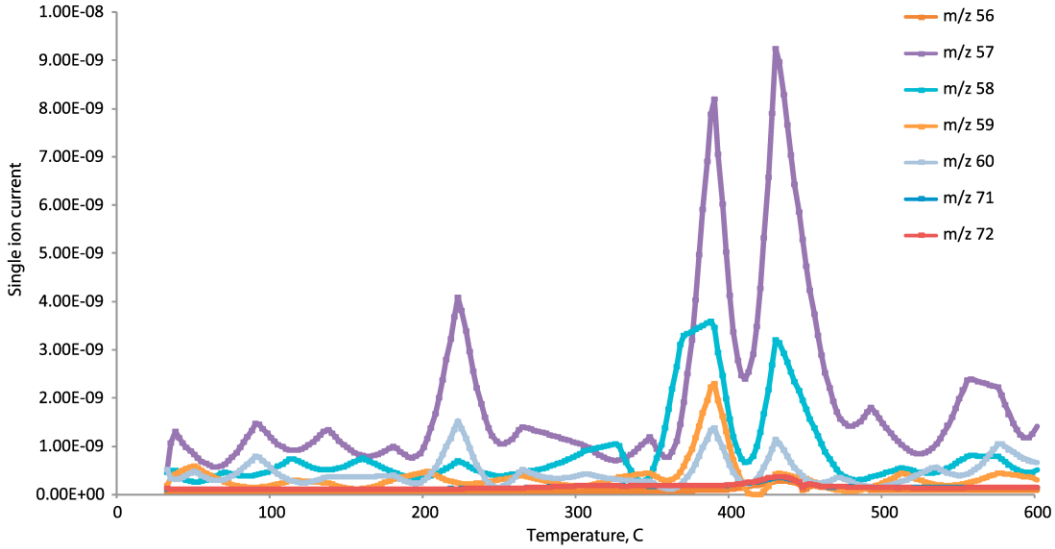

Fig. 9: Tapping Mode AFM Images of a Polyurea–APP

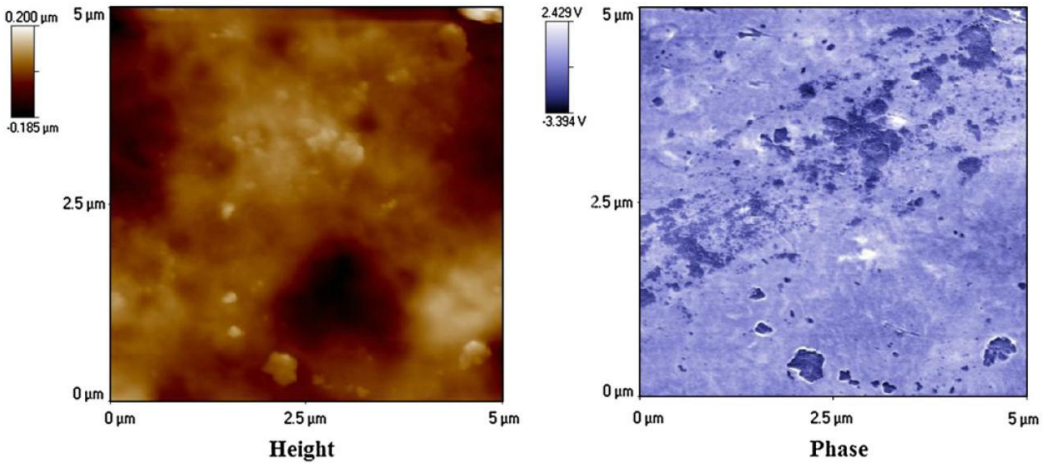

The left image is the height or topographic image, while the right image is the phase contrast image.

Fig. 10: TG and DTG of Polyurea–APP under Nitrogen Atmosphere

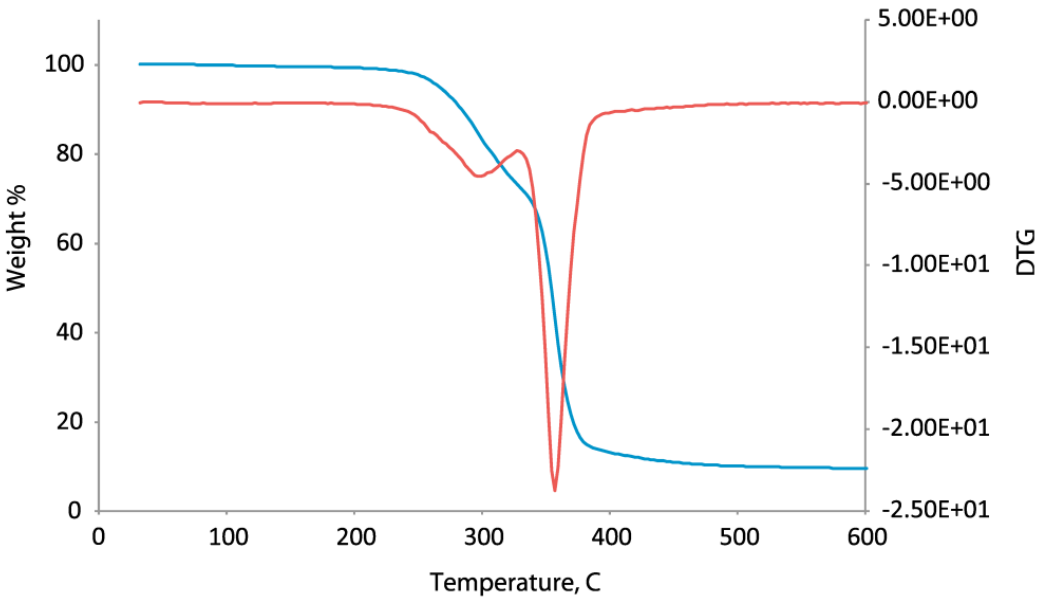

Fig. 11: 3D Diagram Corresponding to Gases Evolved from Degradation of Polyurea/Ammonium Polyphosphate in the Temperature Range 30–600 °C

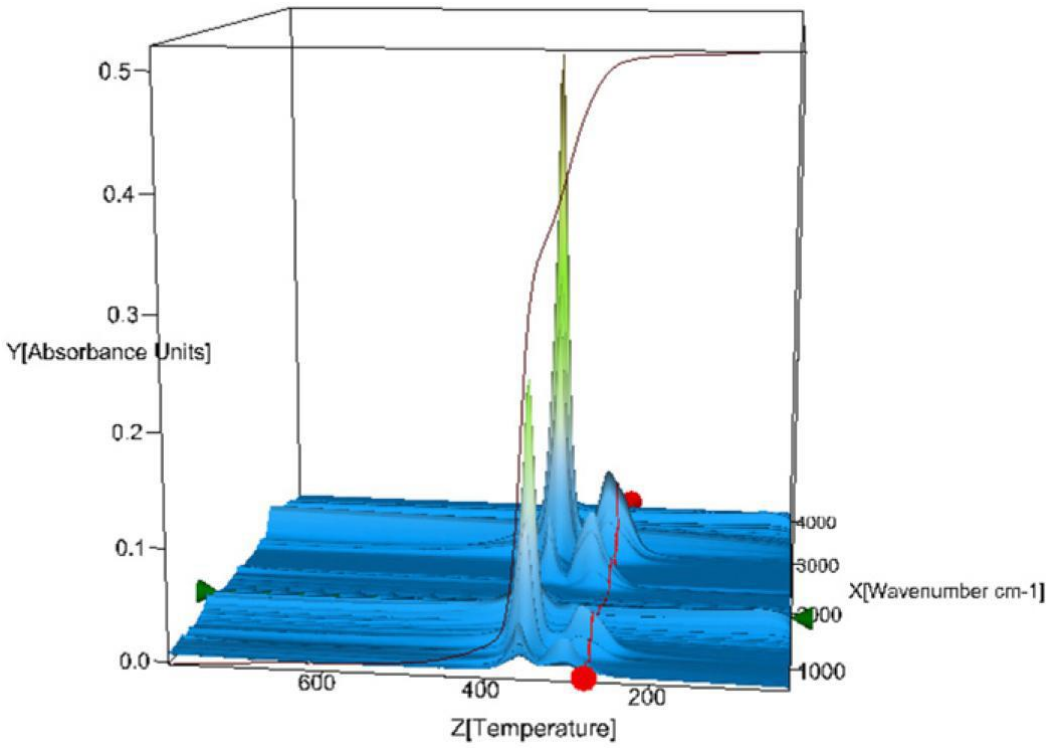

Fig. 12: Single Ion Current Curves for Species Produced from Degradation of Polyurea-APP

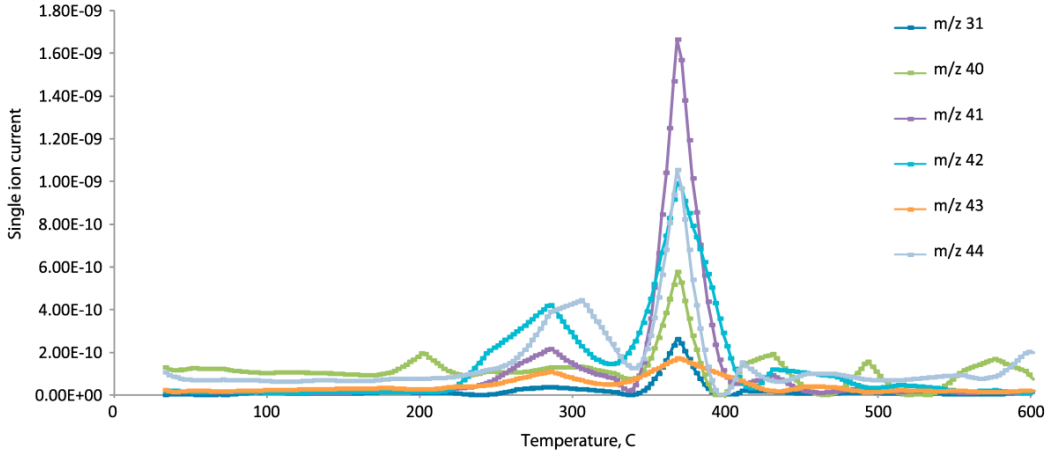

Fig. 13: Single Ion Current Curves for Species Produced from Degradation of Polyurea-APP

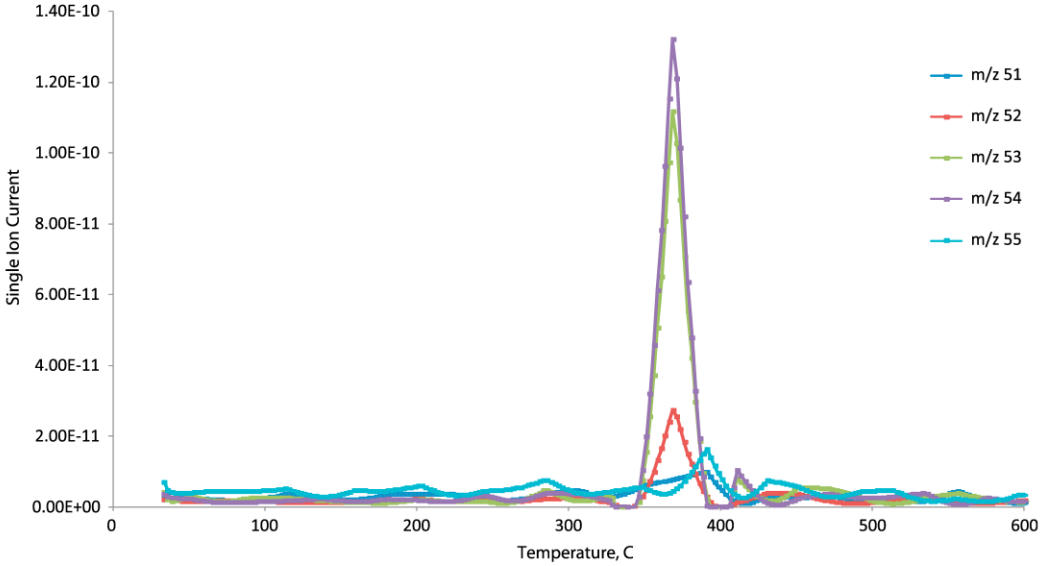

Fig. 14: Single Ion Current Curves for Species Produced from Degradation of Polyurea–APP

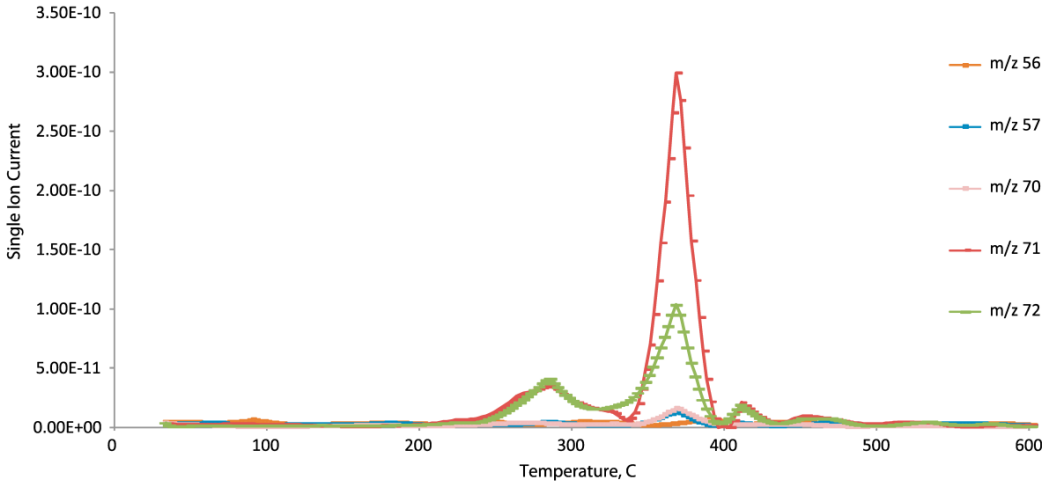

Fig. 15: Tapping Mode AFM Images of a Polyurea–EG

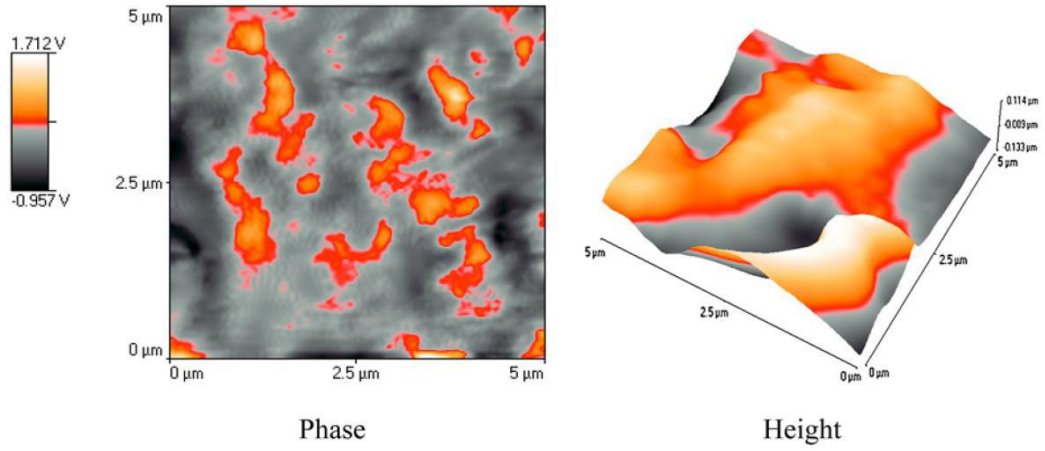

The left image is the phase contrast image while the right image is the height or topgraphic image.

Fig. 16: TG and DTG of Polyurea–EG under Nitrogen Atmosphere

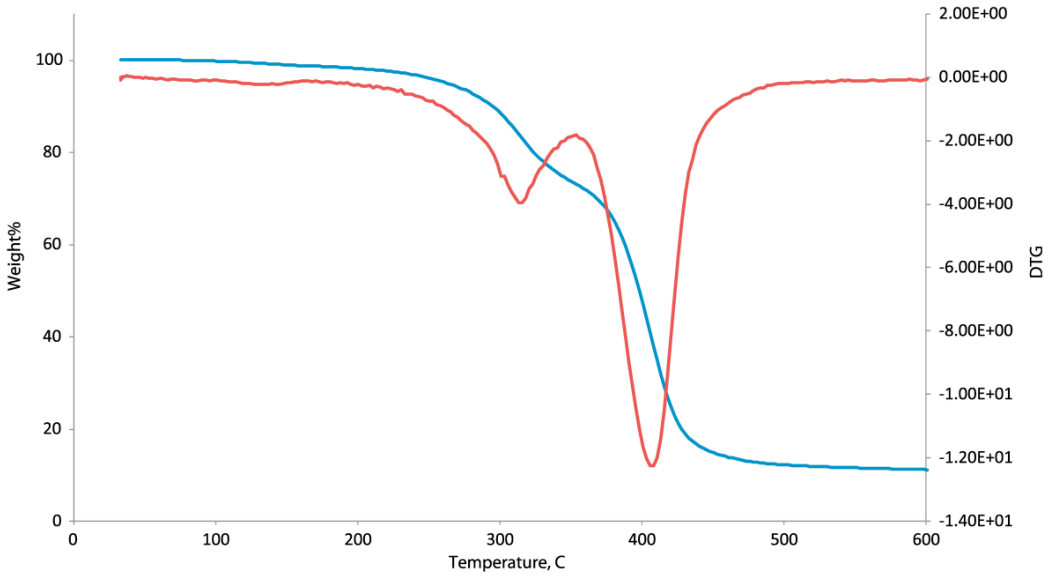

Fig. 17: FTIR of PU–EG Showing Species Evovled during the First and the Second Degradation Steps

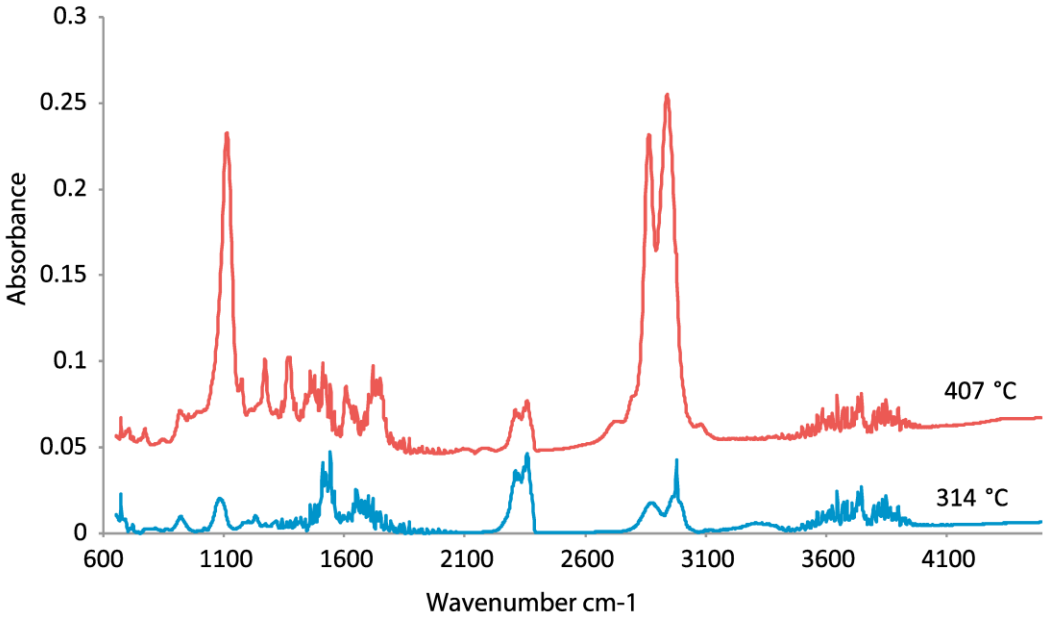

Fig. 18: Total Ion Current of Species Produced in the First Degradation Step of Polyurea with Expandable Graphite

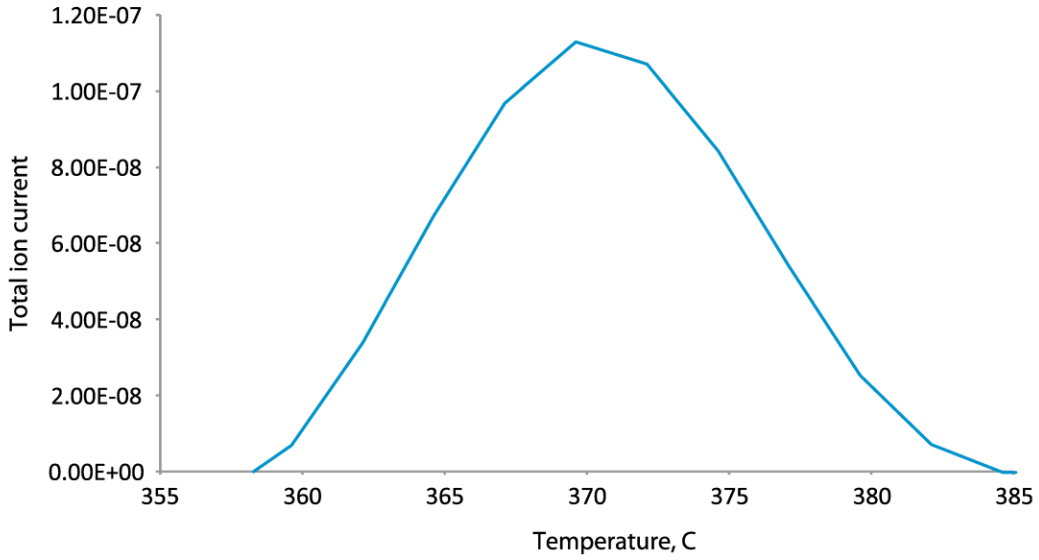

Polymer, Vol. 51, No. 11 (May 2010): pg. 2277-2285. DOI.

Fig. 19: Total Ion Current of Species Produced in the Second Degradation Step of Polyurea with Expandable Graphite